International Journal of Heat and Fluid Flow 31 (2010) 191–200

Contents lists available at ScienceDirect

International Journal of Heat and Fluid Flow

journal homepage: www.elsevier.com/locate/ijhff

Soret and thermosolutal effects on natural convection in a shallow cavity filled with a binary mixture

I. Alloui [a,*], H. Benmoussa [b], P. Vasseur [c]

[a] Université Kasdi Merbah, BP 156 Rouissat, Ouargla 30130, Algeria
[b] Université Hadj Lakhdar, 1 rue Chahid Boukhlouf, Batna 05000, Algeria
[c] Ecole Polytechnique, C.P. 6079, Succ "Center Ville", Montréal, Québec, Canada H3C 3A7

ARTICLE INFO

Article history:
Received 18 April 2009
Received in revised form 26 October 2009
Accepted 30 November 2009
Available online 12 January 2010

Keywords:
Natural convection
Fluid layer
Double diffusion
Soret effect

ABSTRACT

This paper reports an analytical and numerical study of the combined Soret and thermosolutal effects on natural convection in a shallow rectangular cavity filled with a binary mixture. Neumann boundary conditions for temperature and concentration are applied to the horizontal walls of the enclosure, while the two vertical ones are assumed impermeable and insulated. The governing parameters for the problem are the thermal Rayleigh number, Ra_T, the Lewis number Le, the buoyancy ratio φ, the solute flux imposed on the horizontal boundaries j, the Prandtl number Pr, the aspect ratio of the cavity A, and the real number a ($a = 0$ for double diffusive convection and $a = 1$ for the coexistence of double diffusion convection and Soret effect). For convection in an infinite layer ($A \gg 1$), analytical solutions for the stream function, temperature and concentration fields are obtained using a parallel flow approximation in the core region of the cavity and an integral form of the energy and constituent equations. The critical Rayleigh numbers for the onset of supercritical and subcritical convection are predicted explicitly by the present model. A linear stability analysis of the parallel flow model is conducted and the critical Rayleigh number for the onset of Hopf's bifurcation is predicted numerically. Also, results are obtained for finite amplitude convection for which the flow and heat and solute transfers are presented in terms of the governing parameters of the problem. Numerical solutions of the full governing equations are obtained for a wide range of the governing parameters. A good agreement is observed between the analytical model and the numerical simulations.

1. Introduction

Buoyancy-driven flows, in a differentially heated binary liquid mixture, can be found in a wide range of situations. In nature such flows are encountered in the oceans, lakes, solar ponds and the atmosphere. They also are responsible for the geophysics of planets. In industry examples include chemical processes, crystal growth, energy storage, material processing such as solidification, food processing, etc.... For a review of the fundamental work in this area, see Turner (1985), Huppert and Turner (1981), and Platten and Legros (1984).

Convection in a multi-component fluid is considerably more complicated than in pure fluids. This is due to the interplay between convection, solutal diffusion and thermal diffusion. Also, depending on how the temperature and concentration gradients are oriented relative to one another, the dynamics of convection in such fluids can be very different from those driven by thermal buoyancy solely. A review of the literature on this topic indicates that two types of problems, related with the generation of the solutal gradients, have been considered. In the first type of problem, called double diffusive convection, the concentration gradients within the binary mixture are induced by the imposition of given solutal boundary conditions on the system. In the second kind of problem, the concentration gradients are not the consequence of solutal boundary conditions applied on the system. Rather, it is the heat fluxes imposed across initially homogeneous mixtures that induce the solutal gradients. This last situation is referred to as Soret induced convection (cross diffusive problems).

Of particular interest among the studies concerning the first type of problem, namely double diffusive convection in a binary fluid, is the pioneering work of Nields (1967). The onset of motion for thermohaline convection, in an initially motionless horizontal fluid layer heated from the bottom, was predicted by this author on the basis of the linear stability theory. The same problem was reconsidered by Veronis (1968) and Baines and Gill (1969) for various boundary conditions applied on the layer. Non-linear stability theories have also been used by Veronis (1965), Huppert and Moore (1976) and Knobloch and Proctor (1981) to predict the thresholds for finite amplitude convection. The existence of

* Corresponding author.
E-mail address: imene.alloui@gmail.com (I. Alloui).

0142-727X/$ - see front matter © 2009 Elsevier Inc. All rights reserved.
doi:10.1016/j.ijheatfluidflow.2009.11.008

Nomenclature

A	aspect ratio of the enclosure, L'/H'
a	integer number as $a = 0$ or 1
c	dimensionless parameter, $aj + 1$
C_S	dimensionless concentration gradient in x-direction
C_T	dimensionless temperature gradient in x-direction
D	isothermal diffusion coefficient, m^2/s
D'	thermodiffusion coefficient, $m^2/(s\,K)$
g	gravitational acceleration, m/s^2
H'	thickness of enclosure, m
j'	solute flux per unit area, $kg/(m^2\,s)$
k	thermal conductivity, $W/(m\,K)$
L'	length of the enclosure, m
Le	Lewis number, α/D
N	mass fraction of the reference component
N_O	initial mass fraction of the reference component
ΔN	characteristic mass fraction difference of the reference component
Nu	Nusselt number, Eq. (14)
Pr	Prandtl number, ν/α
q'	constant heat flux per unit area, W/m^2
Ra_T	thermal Rayleigh number, $g\beta'_T q' H'^4/k\alpha\nu$
Ra_{TC}	critical thermal Rayleigh number
$\bar{R}_S$	normalized solutal Rayleigh number, $\bar{R}_T \varphi Le$
$\bar{R}_T$	normalized thermal Rayleigh number, $Ra_T/720$
Sh	Sherwood number, Eq. (15)
T	dimensionless temperature, Eq. (7)
t	dimensionless time, Eq. (7)
ΔT	characteristic temperature difference, $q'H'/k$
u	dimensionless velocity x-component, Eq. (7)
v	dimensionless velocity y-component, Eq. (7)
x, y	Cartesian coordinates measured from the center of cavity, Eq. (7)

Greek symbols

α	fluid thermal diffusivity, m^2/s
β_N	mass fraction expansion coefficient
β'_T	thermal expansion coefficient, K^{-1}
ν	fluid kinematic viscosity, m^2/s
φ	buoyancy ratio, $\beta_N \Delta N/\beta'_T \Delta T'$
Ψ	dimensionless stream function, Ψ'/α
ρ	density of fluid, kg/m^3
ω	dimensionless vorticity, $\omega' H'^2/\alpha$

Superscript

$'$	dimensional quantities

Subscripts

o	refers to the value taken at the center of the cavity
c	refers to critical conditions

subcritical convection was reported by these authors. Steady convective motion in a fluid layer with an unstable thermal and a stable salinity stratification has been investigated by Proctor (1981), using a perturbation theory. It was found that, independently of the solutal Rayleigh number, finite amplitude convection can occur at values of the thermal Rayleigh number much smaller than that necessary for infinitesimal oscillations. The onset of thermosolutal convection and finite amplitude flows in a shallow cavity, due to vertical gradients of heat and solute, was investigated analytically and numerically by Mamou et al. (2001). Both Dirichlet and Neumann boundary conditions for temperature and solute concentration, applied on the horizontal walls of the system, are considered. The thresholds for finite amplitude, oscillatory and monotonic convection instabilities are obtained explicitly in terms of the governing parameters. Results indicate that multiple confined steady and unsteady states can coexist. Also, the threshold for Hopf bifurcation was determined. The effect of temperature modulation on the onset of convection in a horizontal fluid layer has been considered by Bhadauria (2006). On the basis of the linear stability theory the stabilizing and destabilizing effects of modulation on the onset of double diffusive convection are discussed.

On the other hand, earlier theoretical investigations on the second type of problems, i.e. Soret induced convection in binary mixtures, were also concerned with the onset of motion in a horizontal fluid layer (see for instance Hurle and Jakeman (1971), Platten and Chavepeyer (1973) and Schechter et al. (1974)). A review of these studies may be found in the book by Platten and Legros (1984). The stability of a triply diffusive fluid layer heated from below has been investigated by Larre et al. (1997). By incorporating the cross diffusion effects in their linear stability of the rest state, the resulting critical parameters for the onset of convection were found to be in agreement with experiments. Soret induced convection in an inclined shallow cavity, filled with a binary fluid, has been investigated by Ouiriemi et al. (2005). For small enough inclinations around the horizontal plane the existence of multiple steady states, for a given set of the governing parameters, was demonstrated analytically and numerically. Ouiriemi et al. (2006) also investigated the case of a horizontal layer of a binary fluid subjected to horizontal gradients of heat and solute. The onset of subcritical convection was predicted for the particular case were the buoyancy forces induced by the thermal and solutal effects are opposing each other and of equal intensity. The onset of Soret driven convective motion in a horizontal fluid layer heated from the top has been analyzed by Kim and Choi (2007), on the basis of the energy method. The stability limits were obtained as a function of the governing parameters of the problem.

All the above studies are concerned with the case of convection, in a horizontal fluid layer, driven either by double diffusion or by the Soret effect. However, in practical applications, there is no reason why these two effects could not be present simultaneously. This paper investigates analytically and numerically the influence of Soret effect on thermosolutal convection within a horizontal layer of fluid. Neumann thermal and solutal boundary conditions are applied on the horizontal walls of the cavity. The paper is organized as follows. In Section 2 the governing equations describing the problem are derived. Section 3 describes the numerical method used to solve the problem. An approximate analytical solution, obtained on the basis of a steady parallel flow approximation, is proposed in Section 4. The results are discussed in Section 5 and a conclusion is presented in Section 6.

2. Mathematical formulation of the problem

Consider the natural convective motion of a binary mixture contained in a shallow two dimensional rectangular cavity. The enclosure, shown in Fig. 1, is of width H' and height L'. The origin of the coordinate system is located at the center of the cavity. Neumann boundary conditions are applied, for both temperature and concentration, on the long side walls of the layer. All the boundaries

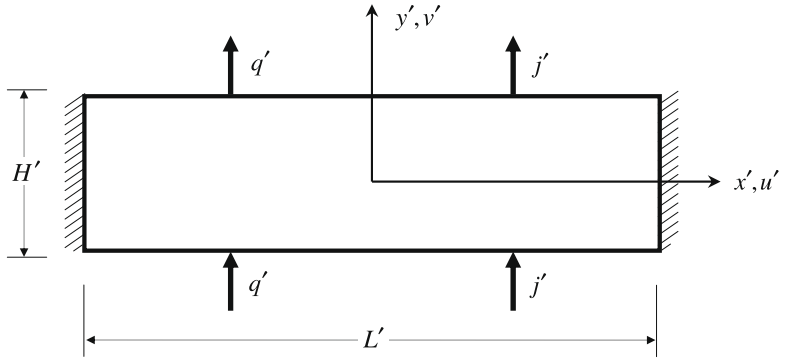

Fig. 1. Schematic diagram of the physical model and coordinate system.

are hydrodynamically impermeable. The binary fluid is assumed to be Newtonian and to satisfy the Boussinesq approximation. The density variation with temperature and concentration is described by the state equation $\rho = \rho_O[1 - \beta'_T(T' - T'_O) - \beta_N(N - N_O)]$ where ρ_O is the fluid mixture density at temperature $T' = T'_O$ and mass fraction of the reference component $N = N_O$. β'_T and β_N are the thermal and concentration expansion coefficients, respectively. The subscript o refers to condition at the origin of the coordinate system. The mass fraction of the denser component of the mixture, N_O, is assumed to be initially uniform.

The phenomenological equations relating the flux of heat $\vec{Q}'$ and matter $\vec{J}'$ to the thermal and solute gradients present in a binary fluid mixture are given by (see for instance, DeGroot and Mazur (1969)):

$$\vec{Q}' = -k\nabla T' \tag{1}$$

$$\vec{J}' = -\rho D\nabla N - a\rho D' N_0(1 - N_0)\nabla T' \tag{2}$$

where a is a real number, the significance of which will be discussed at the end of this section, k and D are the thermal conductivity and the molecular (or isothermal) diffusion coefficient of species and D' the thermodiffusion coefficient. The second term, in the right hand side of Eq. (2), describes the Soret effect i.e. mass separation due to a temperature gradient.

In the present study the Dufour effect, i.e. heat transfer driven by a concentration gradient, is neglected as usual. This parameter can be important in binary gas mixtures but is negligible in binary liquid mixture.

The balanced equations for momentum, energy and mass fraction of the denser components are given below in terms of the vorticity ω', stream function Ψ' and velocity field $\vec{V}'$ as:

$$\frac{\partial\omega'}{\partial t'} + J(\Psi', \omega') = \nu\nabla^2\omega' - \frac{\beta'_T g}{\nu}\frac{\partial}{\partial x'}\left(T' + \frac{\beta_N}{\beta'_T}N\right) \tag{3}$$

$$\frac{\partial T'}{\partial t'} + J(\Psi', T') = \alpha\nabla^2 T' \tag{4}$$

$$\frac{\partial N}{\partial t'} + J(\Psi', N) = D\nabla^2 N + aD' N_0(1 - N_0)\nabla^2 T' \tag{5}$$

where a is a real number, the significance of which will be discussed in the following text, $\omega' = -\nabla^2\Psi'$, $J(f, g) = f_y g_x - f_x g_y$. As usual, we have: $u' = \partial\Psi'/\partial y'$, $v' = -\partial\Psi'/\partial x'$ such that the mass conservation is satisfied. In the above equations, ν is the kinematic viscosity of the mixture and α the thermal diffusivity coefficient. The boundary conditions applied on the wall of the layer are:

$$x' = \pm\frac{L'}{2}, \quad \Psi' = \frac{\partial\Psi'}{\partial x'} = 0, \quad \frac{\partial T'}{\partial x'} = 0, \quad \frac{\partial N}{\partial x'} = 0 \tag{6}$$

$$y' = \pm\frac{H'}{2}, \quad \Psi' = \frac{\partial\Psi'}{\partial y'} = 0, \quad \frac{\partial T'}{\partial y'} = -\frac{q'}{k},$$
$$\frac{\partial N}{\partial y'} = a\frac{j'}{\rho_0 D} - \frac{D'}{D}N_0(1 - N_0)\frac{\partial T'}{\partial y'}$$

Introducing the following dimensionless variables (primed quantities are dimensional)

$$(x, y) = (x', y')/H', \quad (u, v) = (u', v')H'/\alpha, \quad t = t'\alpha/H'^2 \tag{7}$$
$$\Psi = \Psi'/\alpha, \quad T = (T' - T'_0)/\Delta T', \quad \Delta T' = q'H'/k, \quad S = N/\Delta N$$

where $\Delta N = j'/\rho D$ for double diffusive convection and $\Delta N = -N_O(1 - N_O)\Delta T' D'/D$ for Soret driven convection.

In term of the above definitions, the dimensionless governing equations for conservation of momentum, energy and species are given by

$$\frac{\partial\nabla^2\Psi}{\partial t} + J(\Psi, \nabla^2\Psi) = Pr\nabla^4\Psi - PrRa_T\frac{\partial}{\partial x}(T + \varphi S) \tag{8}$$

$$\frac{\partial T}{\partial t} + J(\Psi, T) = \nabla^2 T \tag{9}$$

$$\frac{\partial S}{\partial t} + J(\Psi, S) = \frac{1}{Le}(\nabla^2 S - a\nabla^2 T) \tag{10}$$

The corresponding dimensionless boundary conditions, namely no-slip conditions and constant heat and mass fluxes applied on the boundaries, are:

$$x = \pm A/2, \quad \Psi = \frac{\partial\Psi}{\partial y} = 0, \quad \frac{\partial T}{\partial x} = \frac{\partial S}{\partial x} = 0 \tag{11}$$

$$y = \pm 1/2, \quad \Psi = \frac{\partial\Psi}{\partial x} = 0, \quad \frac{\partial T}{\partial y} = -1, \quad \frac{\partial S}{\partial y} = -c \tag{12}$$

where $c = (aj + 1)$.

In the present formulation the particular case $a = 0$ corresponds to double diffusive convection for which the Soret contribution term on the right hand side of the equation of conservation of species, Eq. (10), disappears. For this situation, considered in the past by Mamou et al. (2001), the solutal buoyancy forces result only from the imposition of the vertical mass fluxes imposed on the horizontal boundaries ($\partial S/\partial y = -1$, Eq. (12)). On the other hand, the case $a = 1$ corresponds to Soret induced convection for which the Soret term on the right hand of Eq. (10) combines with the vertical mass fluxes imposed on the horizontal boundaries ($\partial S/\partial y = -(j + 1)$, Eq. (12)), to give rise to the solutal buoyancy forces. The particular condition $j = 0$ corresponds to a boundary impermeable to the solute. For this situation, which is usually considered in the literature (see for instance Ouiriemi et al. (2005, 2006)), it follows from Eq. (2) that ($\partial S/\partial y - \partial T/\partial y = 0$). However, in general, the boundaries can be permeable to the solute such that the condition $j \neq 0$, applies as considered in the present study. This type of boundary

condition has been considered recently, for the first time, by Bennacer et al. (2003).

In Eqs. (8)–(12), one notice the presence of seven governing parameters, namely the thermal Rayleigh number Ra_T, the Lewis number Le, the buoyancy ratio φ, the solute flux imposed on the horizontal boundaries j, the Prandtl number Pr, the aspect ratio of the enclosure A, and the parameter a, defined as

$$Ra_T = \frac{\beta'_T g q' H'^4}{k\alpha\nu} \quad \varphi = \frac{\beta_N \Delta N}{\beta'_T \Delta T'} \quad j = \frac{j' H'}{\rho_0 D \Delta N}$$
$$Pr = \frac{\nu}{\alpha} \quad Le = \frac{\alpha}{D} \quad A = \frac{L'}{H'} \tag{13}$$

where α is the thermal diffusivity and ν the kinetic viscosity of fluid.

In the buoyancy ratio φ it is noticed that, for most of the fluids at ordinary temperature and pressure β'_T is positive but β_N can be positive or negative according to the contribution of the diffusing components to the fluid density. In the present study β_N is supposed positive, i.e. $\varphi > 0$ for aiding flows and $\varphi < 0$ for opposing flows.

The heat and mass transfer rates, expressed in terms of the Nusselt and Sherwood numbers, can be computed from the following expressions:

$$Nu = \frac{q'}{k\Delta T'/H'} = \frac{1}{\Delta T} \tag{14}$$

$$Sh = \frac{j'}{D\Delta N/H'} = \frac{c}{\Delta S} \tag{15}$$

where $\Delta T = T(0, -1/2) - T(0, 1/2)$ and $\Delta S = S(0, -1/2) - S(0, 1/2)$ are the temperature and concentration differences, evaluated at $x = 0$. This follows from the fact that ΔT and ΔS are x independent such that they are arbitrary evaluated at the geometrical center of the cavity. The parameter c in Eq. (15), follows from the fact that it is required that $Sh = 1$ when the fluid is at rest ($\Psi = 0$). Eqs. (8)–(10), together with the boundary conditions (11) and (12) then completely determine the problem in terms of the governing parameters (13). In the following sections both numerical and analytical solutions are discussed.

3. Numerical solution

The solution of the governing equations and boundary conditions, Eqs. (8)–(10), is obtained using a control volume approach and SIMPLER algorithm (Patankar 1980). A finite difference procedure with variable grid size is considered for better consideration of boundary conditions. The power-law scheme, described by Patankar in his book, is used to evaluate the flow, heat and mass fluxes across each of the control volume boundaries. A second order backwards finite difference scheme is employed to discretize the temporal terms appearing in the governing equations.

A line-by-line tridiagonal matrix algorithm with relaxation is used in conjunction with iterations to solve the non-linear discretized equations. We consider that convergence is reached when

$$\frac{\sum_i \sum_j |\Psi_{ij}^{n+1} - \Psi_{ij}^{n}|}{\sum_i \sum_j |\Psi_{ij}^{n+1}|} \leqslant 10^{-6} \tag{16}$$

where the superscripts n and $(n+1)$ indicate the value of the nth and $(n+1)$th iterations respectively, i and j indices denote grid location in the (x, y) plane.

As mentioned above the present problem depends upon the parameters Ra_T, φ, j, Le, Pr, c, A and a. The numerical results presented in this study were obtained for $A = 6$. Such an aspect ratio is large enough to approximate the parallel flow model describe in the following section (see Ouiriemi et al. (2006)). Numerical tests, using various mesh sizes, were done for the same conditions in order to determine the best compromise between accuracy of the results and computer time. Thus, most of the calculations presented in this paper were performed using a 60×180 grid. The criteria of convergence are to conserve momentum, energy and species globally and to insure convergence of pre-selected dependent variables to constant values within machine error at each time step.

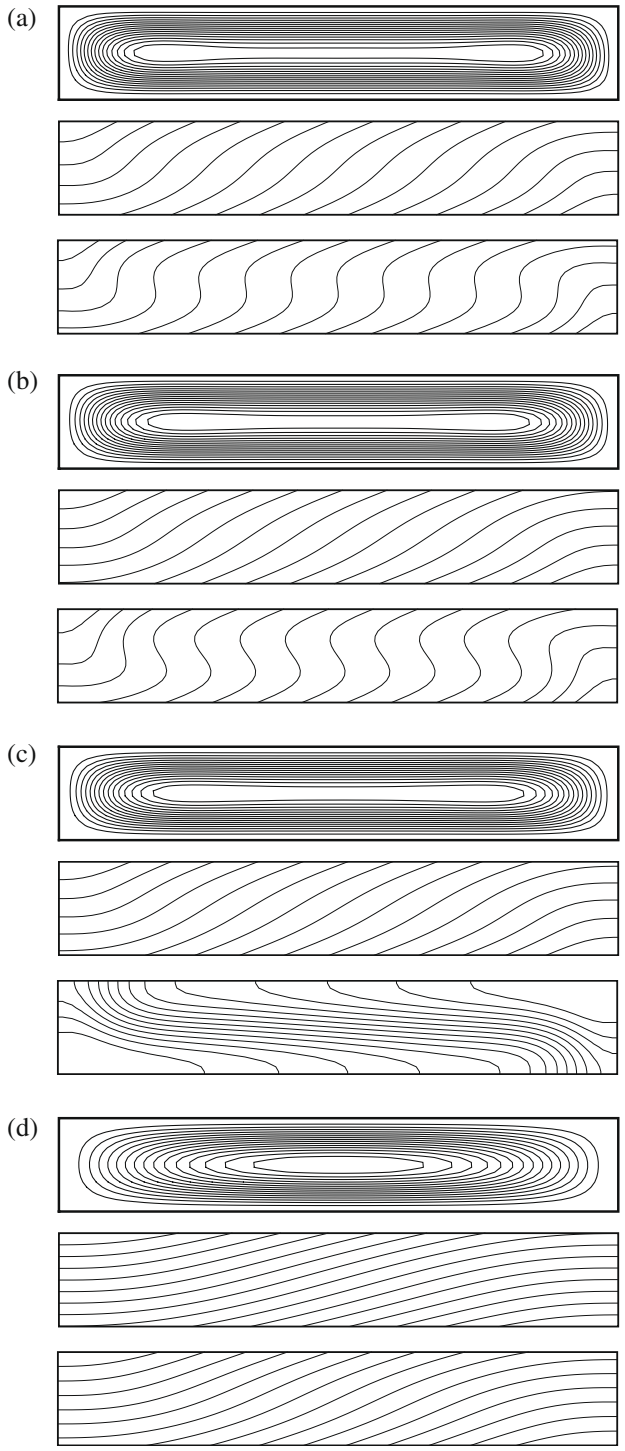

Fig. 2. Contour lines of stream function (top), temperature (middle) and concentration (bottom) predicted by the numerical solution of the full governing equations for $Ra_T = 10^3$, $Le = 2$, $\varphi = 0.05$, $a = 1$ and: (a) $j = 5$, $\Psi_{max} = 1.40$, $Nu = 1.43$, $Sh = 2.28$, (b) $j = 0$, $\Psi_{max} = 1.29$, $Nu = 1.29$, $Sh = 3.20$, (c) $j = -1$, $\Psi_{max} = 1.01$, $Nu = 1.25$ and (d) $j = -4$, $\Psi_{max} = 0.50$, $Nu = 1.07$, $Sh = 1.56$.

All the numerical results presented in this study are limited to water-based solutions, i.e. $Pr = 7$. As discussed by many authors, see for instance Trevisan and Bejan (1985), the present solution is rather independent of this parameter provided that this latter is of order one or greater. Furthermore, this point is confirmed by the analytical solution discussed in the following section which, in its range of validity, is independent of Pr.

Typical numerical results are presented in Fig. 2a–d for $Ra_T = 10^3$, $Le = 2$, $\varphi = 0.05$, $A = 6$, $a = 1$ and various values of j. On the graphs, streamlines, isotherms and isoconcentrates are presented from top to bottom. For each map of Fig. 2, the increments between adjacent streamlines, isotherms and isoconcentrates are $\Delta\xi = (\xi_{max} - \xi_{min})/15$, where ξ stands for Ψ, T and N, and ξ_{max} and ξ_{min} are the maximum and minimum values of ξ, respectively. The effects of varying the intensity of solute flux j from 5 to -4, on the strength of convection (Ψ_{max}) and the resulting heat (Nu) and solute transfer (Sh) are observed to be considerable. This point will be discussed in detail in the following sections. However, Fig. 2a–d clearly illustrate the fact that for a shallow cavity ($A \gg 1$) the flow in the core of the enclosure is essentially parallel while the temperature and concentration are linearly stratified along the x-direction. The numerically determined profiles of horizontal velocity u at the center of the convective cell are compared in Fig. 3 with their analytical counterparts derived below. The agreement between the two solutions is seen to be excellent. It is noted from Fig. 3 that the rest state, within the convective cell, is reached when $j \leqslant -4.30$. This follows from the fact that for the parameters considered here, namely $Le = 2$, $\varphi = 0.05$ and $a = 1$, the critical Rayleigh number for the onset of motion is given by $Ra_{TC}^{sup} \geqslant 1000$, as predicted by Eq. (24).

4. Analytical solution

In the limit of a shallow cavity $A \gg 1$, the governing equations (8)–(10) can be considerably simplified under the parallel flow approximation $\Psi(x, y) \approx \Psi(y)$, $T(x, y) \approx C_T x + \theta_T(y)$ and $S(x, y) \approx C_S x + \theta_S(y)$, where C_T and C_S are unknown constant temperature and concentration gradients respectively in x-direction. The procedure to obtain the analytical solution presented in this section has already been described in details (see for instance Mamou et al., 2001), such that only the final results are presented here.

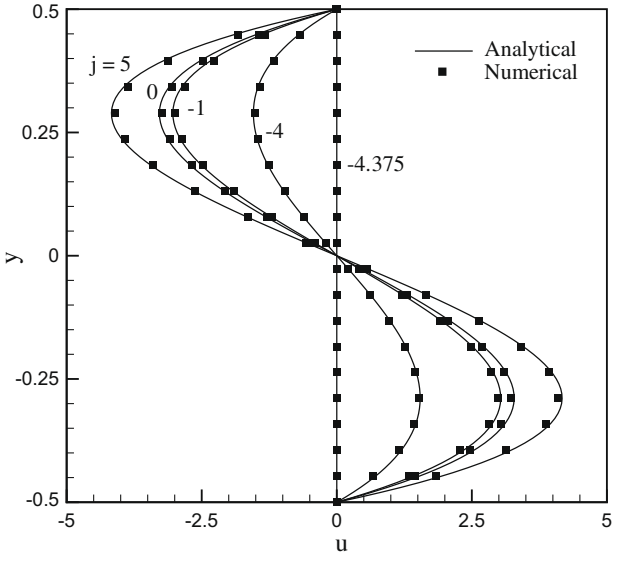

Fig. 3. Effect of parameter j on the horizontal velocity profiles for $Ra_T = 10^3$, $Le = 2$, $\varphi = 0.05$ and $a = 1$. — analytical; ● numerical.

Thus, upon substituting the above approximations for Ψ, T and S into Eqs (8)–(10) and resolving the resulting ordinary differential equations, under the appropriate boundary conditions, it is found that the stream function and the temperature and concentration fields are given by:

$$\Psi(y) = \Psi_0(4y^2 - 1)^2 \tag{17}$$

$$T = C_T x + \frac{C_T \Psi_0}{15} y(48y^4 - 40y^2 + 15) - y \tag{18}$$

$$S = C_S x + \frac{(aC_T + LeC_S)\Psi_0}{15} y(48y^4 - 40y^2 + 15) - cy \tag{19}$$

with $\Psi_0 = Ra_T(C_T + \varphi C_S)/384$.

In the above equations C_T and C_S are given by:

$$C_T = \frac{I_1}{1 + I_2}, \quad C_S = \frac{(1 - I_2 Le)aC_T + cI_1 Le}{1 + I_2 Le^2} \tag{20}$$

where $I_1 = 8\Psi_0/15$ and $I_2 = 128\Psi_0^2/315$.

The value of the stream function at the center of the cavity can be evaluated from the following expression:

$$\Psi_0 = \left\{ \pm \frac{\sqrt{b}}{Le} \left[d_1 \pm \sqrt{d_1^2 + d_2} \right]^{1/2}, 0 \right\} \tag{21}$$

where

$$\begin{aligned} d_1 &= \bar{R}_T Le[Le + \varphi(c - a)] - (Le^2 + 1) \\ d_2 &= 4\bar{R}_T Le^2[1 + \varphi(cLe + a)] - 4Le^2 \\ \bar{R}_T &= Ra_T/Ra^{sup} \quad Ra^{sup} = 720 \end{aligned} \tag{22}$$

and $b = 315/256$. It is noted that the value $Ra^{sup} = 720$ corresponds to the onset of motion predicted in the past by Sparrow et al. (1964).

Eq. (21) indicates that five solutions are possible. One of these solutions, namely $\Psi_0 = 0$, corresponds to the rest state. The first signs + and – correspond to counterclockwise and clockwise unicellular circulations, respectively. Within the square root, the + and – signs refer to stable and unstable convection flows, respectively. As indicated by Eq. (21) the rest state is a possible solution. However it is well known that, above given critical values, a transition to a convective regime occurs. In the case of a binary mixture two types of bifurcations are possible.

The first one, characterized by a transition from the quiescent state to convection regime occurring through zero flow amplitude ($\Psi_0 = 0$) is obtained at a supercritical Rayleigh number Ra_{TC}^{sup}, which is predicted from Eq. (21) when the conditions $d_1 < 0$ and $d_2 = 0$ are satisfied, as

$$Ra_{TC}^{sup} = \frac{720}{1 + \varphi(cLe + a)} \tag{23}$$

In the present analysis, it can be demonstrated that subcritical flows with finite amplitude convection occur when $d_1 > 0$ and $d_1^2 + d_2 = 0$, at a subcritical Rayleigh number given by:

$$\begin{aligned} Ra_{TC}^{sub} = \frac{720(1 + Le)}{Le[Le + \varphi(c - a)]^2} \times [&(Le - 1)(Le - \varphi c) - a\varphi(Le + 1) \\ &+ 2\sqrt{\varphi Le(cLe + a - c)(a\varphi - Le + 1)}] \end{aligned} \tag{24}$$

At the threshold Ra_{TC}^{sub}, the flow intensity is:

$$\Psi_0 = \pm \frac{\sqrt{bd_1}}{Le} \tag{25}$$

The above results indicates that the occurrence of subcritical is related to j, Le and φ. Thus, from the conditions $d_1 = 0$ and $d_2 = 0$ the following specific conditions for the transition between supercritical and subcritical flows can be derived in terms of the following critical Lewis number Le_c:

$$Le_c = \left[-a \pm \sqrt{a^2 + 4c(-1/\bar{R}_S + c - a)}\right]/2c \tag{26}$$

where $\bar{R}_S = \bar{R}_T \varphi Le$ and $\bar{R}_T$ is given by

$$\bar{R}_T = \frac{cLe^3 + a(Le^2 + Le + 1)}{Le[c(Le^2 - 1) + a(Le + 1)]}. \tag{27}$$

The local heat and mass transfer rates are obtained according to Eqs. (14), (15), (18), and (19). It is readily found that:

$$Nu = \frac{10}{3}\left(\frac{\Psi_0^2 + 2b}{\Psi_0^2 + \frac{20}{3}b}\right) \tag{28}$$

$$Sh = \frac{Sh_0}{1 - \Omega Sh_0(Nu - 1)/Nu} \tag{29}$$

where:

$$Sh_0 = \frac{10}{3}\left(\frac{Le^2\Psi_0^2 + 2b}{Le^2\Psi_0^2 + \frac{20}{3}b}\right) \quad \text{and} \quad \Omega = \frac{2ab(Le + 1)}{Le^2\Psi_0^2 + 2b}.$$

The above analytical model is valid asymptotically in the limit of both $A \gg 1$ and $\mathrm{Pr} \gg 1$. Furthermore, the following discussion is limited to the case $a = 1$, corresponding to Soret induced convection in a fluid layer subjected to the imposition, on the horizontal boundaries, of a constant solute flux j. The case $a = 0$, as already discussed, has been investigated in the past by Mamou et al. (2001) and is not considered here. It follows that the resulting problem is now governed by only four parameters, namely the thermal Rayleigh number Ra_T, the mass flux j, the buoyancy ratio φ and the Lewis number Le.

Typical bifurcation diagrams are presented in Figs. 4 and 5 for various values of the solute flux j, for $Le = 10$ and $\varphi = 0.05$ and $\varphi = -0.05$, respectively. The thermal Rayleigh number is normalized with respect to the critical parameter for the onset of pure thermal convection, namely $Ra^{sup} = 720$. The curves presented in graphs are the result of the present analytical model, the solid (dotted) lines corresponding to stables (unstable) branches (see for instance Mamou and Vasseur (1999)). The numerical solution of the full governing equations, depicted by dots, is observed to be in excellent agreement with the analytical model.

Fig. 4a illustrates the effect of $\bar{R}_T$ on Ψ_0 for values of $2 \geqslant j \geqslant -4$ when φ is greater than zero, namely $\varphi = 0.05$. Pure Soret induced convection can be recovered by substituting $j = 0$ in Eqs. (17)–(22). For this situation, both thermal and solutal contributions are destabilizing ($\bar{R}_T > 0$ and $\varphi > 0$). As a result the onset of convection occurs at $\bar{R}_{TC}^{sup} = 0.645$, Eq. (23), through a pitchfork bifurcation. Upon applying a solute flux $j > 0$ on the system both Soret and double diffusive effects contribute to destabilize the system. Thus, as exemplified by the curve $j = 2$, the onset of convection occurs at a lower supercritical Rayleigh number, namely $\bar{R}_{TC}^{sup} = 0.392$. On the other hand, as the value of j is made smaller than zero, the double diffusion effects induced by the solute flux are progressively stabilizing the system in opposition with the destabilizing contributions of the thermal and Soret ones. It is well known that, for this situation, the onset of motion can occur with finite amplitude convection at a subcritical thermal Rayleigh number predicted by Eq. (24). The specific conditions for the transition between supercritical and subcritical flows, given by Eq. (26), can be expressed explicitly in terms of the critical solute flux as j_c

$$j_c = -\frac{1 + \varphi[Le^3 + a(Le^2 + Le + 1)]}{a\varphi Le^3}. \tag{30}$$

From the above equation it is found that the transition occurs at $j_c = -1.1\,3$ and the resulting curve is plotted in Fig. 4a for reference. Thus, for values of j below the critical value j_c, $\bar{R}_{TC}^{sub} = 1.14$ when

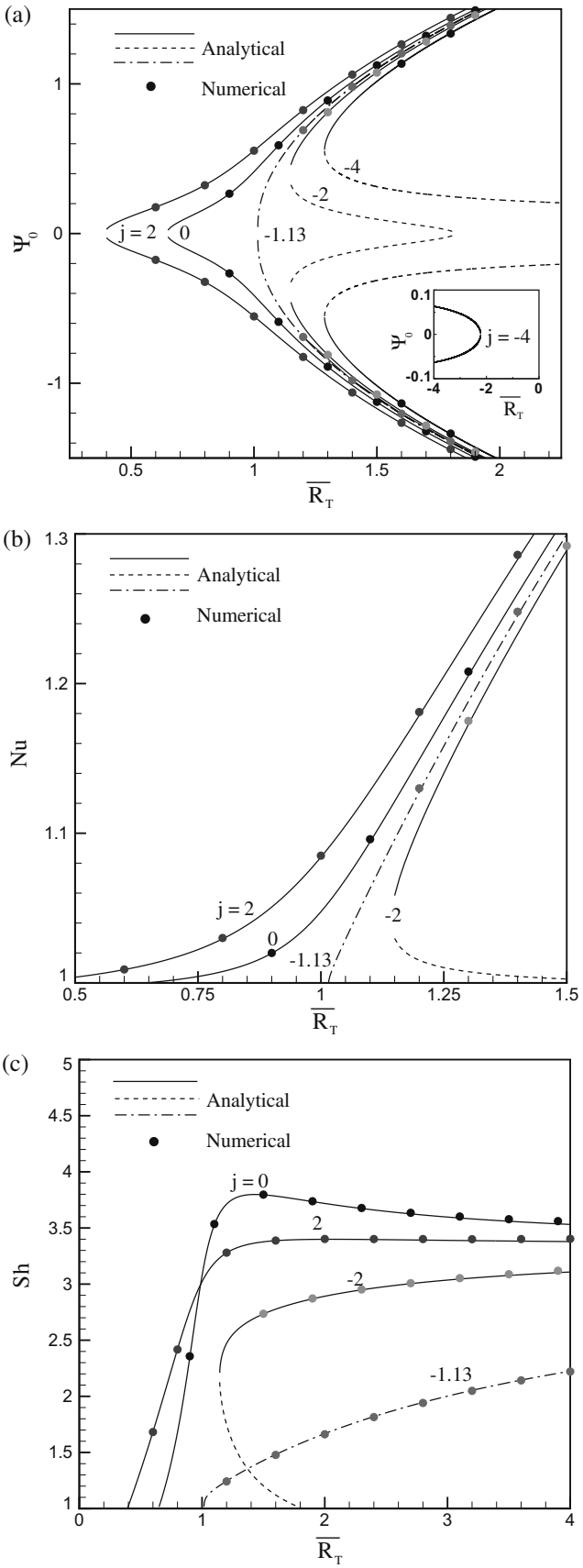

Fig. 4. Bifurcation diagrams as a function of $\bar{R}_T$ for $Le = 10$, $\varphi = 0.05$ and various values of j: (a) flow intensity Ψ_0, (b) Nusselt number Nu and (c) Sherwood number Sh. —, —, analytical; ● numerical.

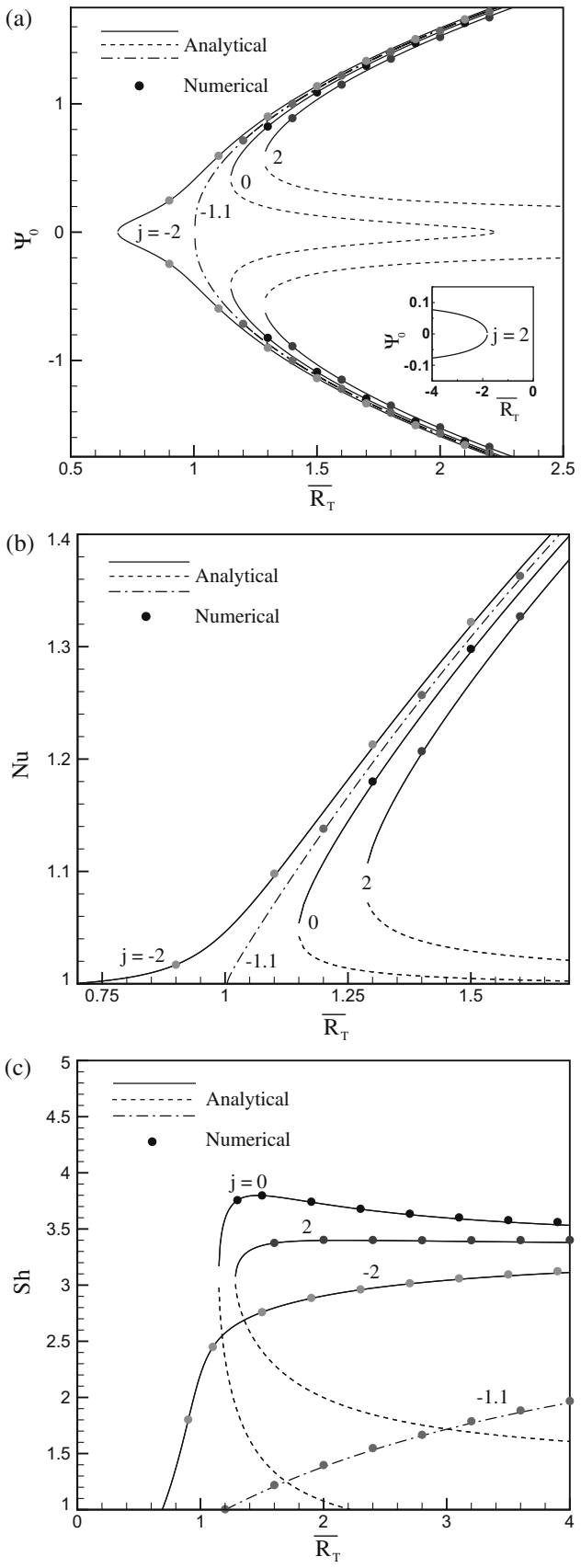

Fig. 5. As Fig. 4, but for $\varphi = -0.05$.

$j = -2$ and $\bar{R}_{TC}^{sub} = 1.29$ when $j = -4$. These points correspond to saddle-node bifurcations, where two branches emerge. An unstable branch, represented by a dashed line, connects the subcritical Rayleigh number $\bar{R}_{TC}^{sub}$ to the supercritical Rayleigh number. The other branch, represented by a solid line, is stable and its existence is confirmed by the numerical results of the full governing equations. The curve $j = -4$ is characterized by the fact that $\bar{R}_{TC}^{sup} = -2.22$. A negative Rayleigh number corresponds to an inversion of the direction of the heat fluxes imposed on the fluid layer such that the thermal contributions are now stabilizing. As a result, upon decreasing $\bar{R}_T$ below the critical value, $\bar{R}_{TC}^{sup} = -2.22$, Fig. 4a indicates the existence of a supercritical bifurcation transition, as exemplified by the curve obtained for $j = -4$.

Fig. 5a illustrates the effects of $\bar{R}_T$ on Ψ_0 obtained for $\varphi = -0.05$, i.e. when φ is smaller than zero. For this situation the thermal buoyancy forces are destabilizing (stabilizing) for $\bar{R}_T > 0$ (<0). However, since $\varphi < 0$ it follows that the Soret effects are stabilizing (destabilizing) for $\bar{R}_T > 0$ (<0) while the double diffusive effects are stabilizing (destabilizing) for $j > 0$ (<0). The transition curve, between supercritical and subcritical convection, occurring at $j = -1.1$ 0, Eq. (30), is plotted on the graph for reference. For $\bar{R}_T < 0$ the occurrence of supercritical convection is possible. Such a bifurcation is illustrated in Fig. 5a for the case $j = 2$.

Figs. 4 and 5 also exemplify the effects of $\bar{R}_T$, φ and j on the heat and mass transfer. Thus, it is observed from Figs. 4b and 5b that, when compared with the pure Soret induced convection situation ($j = 0$) the Nusselt number Nu is higher for $j > 0$, for which the Soret and double diffusive effects add to the thermal effects to destabilize the layer. Conversely, the Nusselt number is lower for $j < 0$ for which the destabilizing thermal influences competes with the stabilizing Soret and double diffusive effects. For very large values of $\bar{R}_T$ it is found from the present theory that both Nu and Sh tend asymptotically (not illustrate on the graphs) towards the limit $Nu = Sh = 10/3$, as it can be deduced from Eqs. (28) and (29). This behavior is a consequence of the particular boundary conditions considered here.

Results obtained for the mass transfer are depicted in Figs. 4c and 5c. It is observed that, for both $\varphi > 0$ and $\varphi < 0$, the Sherwood number for Soret induced convection ($j = 0$) is found to be greater than obtained for $j \neq 0$, i.e. under the combined influences of Soret and double diffusive effects. However, it is noticed that the significance of Sh for these two cases is different. The Sherwood number for double diffusive convection ($j \neq 0$), represents the mass transfer across the horizontal boundaries of the layer resulting from the combined action of convection and conduction. On the other hand, the Sherwood number for Soret induced convection has not the same interpretation since the boundaries of the layer are impermeable ($j = 0$). Thus, for this situation, Sh is rather related to the concentration distribution induced by the Soret effect and by convection.

Another view of the effects of aiding and opposing thermal and solutal buoyancy forces is presented in Fig. 6a–b in terms of Ψ_0 versus j and $\bar{R}_T$, for $Le = 10$ and $\varphi = 0.5$ and -0.5, respectively. The case $\bar{R}_T > 0$, for which the thermal buoyancy forces (heat flux applied at the bottom of the layer), have a destabilizing effect will be first discussed. For this situation, for $\varphi > 0$ ($\varphi < 0$), the solutal buoyancy forces induced by the Soret effect are destabilizing (stabilizing). Similarly, those induced by the mass flux are destabilizing (stabilizing) for $j > 0$ ($j < 0$). Naturally, the net solutal buoyancy forces result from the addition of these two contributions .Thus, it is seen that for $\varphi > 0$, Fig. 6a, that the onset of motion occurs through a supercritical bifurcation for $j > 0$ since both the thermal and the solutal forces are destabilizing. This situation is exemplified by the curve for $\bar{R}_T = 0.1$. On the other hand, upon decreasing j below zero the contribution of the mass flux over the Soret effect becomes progressively more important such that the net solutal buoyancy forces

become eventually stabilizing. As discussed in details by Mamou and Vasseur [29], when the thermal and solutal forces are opposing each other the resulting onset of motion occurs through a subcritical bifurcation, see the curve for $\bar{R}_T = 2$, provided that the stabilizing agent is the slower diffusing component ($Le > 1$).The transition curve between supercritical and subcritical bifurcations, as predicted by Eqs. (30), namely $\bar{R}_T = 1.069$ is presented in the graph for reference. Similarly, Fig. 6(b) shows that for $\varphi < 0$ the transitions curve between supercritical and subcritical bifurcations, as predicted by Eqs. (30), occurs now at $\bar{R}_T = 0.957$. For lower (higher) values of $\bar{R}_T$ subcritical (supercritical) bifurcations are possible for $j > 0$ ($j < 0$).In Fig. 6a–b results are also presented for $\bar{R}_T < 0$, for which the direction of the heat and mass fluxes, in Fig. 1, are reversed. Thus, the heat flux applied on the top of the layer is now stabilizing and the only way to observed motion is to create a destabilizing net solutal buoyancy force. Typical results are presented for $\bar{R}_T = -2$, in Fig. 6a–b, and it observed that the resulting bifurcations are supercritical since that for this situation the stabilizing agent is not anymore the slower diffusing component.

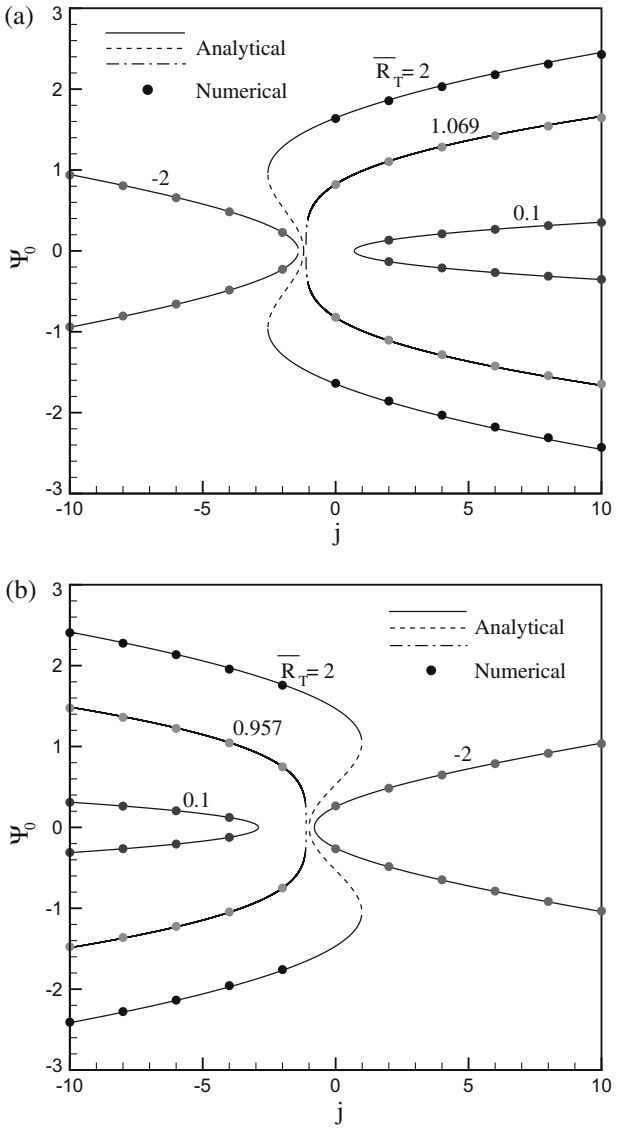

Fig. 6. Bifurcation diagrams in terms of Ψ_0 versus j and $\bar{R}_T$ for $Le = 10$, a = 1and for: (a) $\varphi = 0.5$ and (b) $\varphi = -0.5$.

5. Linear stability analysis

In this section, the stability of the parallel flow pattern, derived in the present study, is examined on the basis of the linear stability theory. It is expected that, upon increasing the intensity of the steady unicellular flow, this latter will become eventually unstable. The transition occurs via a Hopf's bifurcation, at a critical Rayleigh number, Ra_{TC}^{Hopf}, which depend upon the value of the governing parameters, namely φ, j, Le, Pr and a. The procedure for the linear stability analysis is well known such that only the main points of the mathematical steps that lead to the solution of the problem are presented here.

At the very beginning of instability, the global flow can be assumed to be a superposition of the basic flow [$\Psi(x, y) \approx \Psi(y)$, $T(x, y) \approx C_T x + \theta_T(y)$ and $S(x, y) \approx C_S x + \theta_S(y)$, as given by Eqs (17)–(22)] and an infinitesimal perturbation. Thus, we have:

$$\left.\begin{aligned} \hat{\psi}(t,x,y) &= \tilde{\psi}(y)e^{pt+ikx} \\ \hat{\theta}_T(t,x,y) &= \tilde{\theta}_T(y)e^{pt+ikx} \\ \hat{\theta}_S(t,x,y) &= \tilde{\theta}_S(y)e^{pt+ikx} \end{aligned}\right\} \tag{31}$$

where $p = \sigma + i\omega$ is the complex amplification rate of the perturbation, k is the real wave number and ω the frequency.

Substitution of the sum of the base flow and perturbation variables, into the set of governing Eqs. (8)–(10), followed by linearization to first-order in small quantities, yields the following system of equations:

$$\mathrm{Pr}(D^4 + k^4)\tilde{\psi} - ikD^3\psi\tilde{\psi} + ik(D^2 - k^2)D\psi\tilde{\psi} - ik\mathrm{Pr}Ra_T(\tilde{\theta}_T + \varphi\tilde{\theta}_S)D\tilde{\psi} = p(D^2 - k^2)\tilde{\psi} \tag{32}$$

$$(D^2 - k^2)\tilde{\theta}_T - ikD\psi\tilde{\theta}_T - C_T D\tilde{\psi} + ikD\theta_T\tilde{\psi} = p\theta_T \tag{33}$$

$$\frac{1}{Le}(D^2 - k^2)(\tilde{\theta}_S - a\tilde{\theta}_T) - ikD\psi\tilde{\theta}_S - C_S D\tilde{\psi} + ikD\theta_S\tilde{\psi} = p\theta_S. \tag{34}$$

From Eqs. (11) and (12) the corresponding boundary conditions are now given

$$y = -1/2, \quad \tilde{\psi} = 0; \quad D^2\tilde{\psi} = 0; \quad D\tilde{\theta}_T = D\tilde{\theta}_S = 0 \tag{35}$$

$$y = 1/2, \quad \tilde{\psi} = 0; \quad D^2\tilde{\psi} = 0; \quad D\tilde{\theta}_T = D\tilde{\theta}_S = 0 \tag{36}$$

where $D = d/dy$.

The perturbed state Eqs. (32)–(34) with the boundary conditions (35) and (36) may be written in a compact matrix form as:

$$L(k)\mathbf{Y} = pM(k)\mathbf{Y} \tag{37}$$

where $\mathbf{Y} = [\tilde{\psi}, \tilde{\theta}_T, \tilde{\theta}_S]$ is a three-component vector of the perturbation and $L(k)$ and $M(k)$ are two linear differential operators that depend on the control parameters Ra_T, φ, Le, Pr , a and j.

The set of Eq. (37) is solved using a finite differences scheme. The system is discretized using a fourth-order scheme in the domain between $y = -1/2$ and $y = 1/2$. For N computational points, the resulting discrete system has $3N$ eigenvalues that can be found using a standard IMSL subroutine such as DGVCCG.

The validation of the present stability analysis can be made for the case considered by Prud'homme and Hung Nguyen (2002) for the particular case of pure fluid layer ($\varphi = 0$). The critical values obtained by these authors, displayed in Table 1, are observed to be in excellent agreement with the results of the numerical procedure described above.

It is noted that, for the special case $\Psi = 0$, $T = -y$ and $S = -cy$, the present procedure yields the supercritical Rayleigh number Ra_{TC}^{sup}, for the onset of motion from the rest state.

Fig. 7 illustrates the influence of j on the critical Rayleigh number $\bar{R}_{TC}$ for the case $\varphi = 0.2$, $Le = 10$ and $a = 1$. In this graph the curves corresponding to the critical Rayleigh numbers, $\bar{R}_{TC}^{sup}$ and

Table 1
Validation of the numerical code, for $\varphi = 0$, in terms of Ra_{TC}^{Hopf}, k_C and ω_C.

Pr	Prud'homme and Hung Nguyen (2002)			Present work		
	Ra_{TC}^{Hopf}	k_C	ω_C	Ra_{TC}^{Hopf}	k_C	ω_C
50	64275.9	4.626	183.9	64275.86	4.626	183.9
100	65125.8	4.662	187.1	65125.75	4.662	187.1
500	65819.3	4.691	189.8	65819.27	4.691	189.8
5000	65977.0	4.697	190.4	65976.98	4.697	190.4

$\bar{R}_{TC}^{osc}$, are the predictions of the linear stability study of the rest state. The subcritical Rayleigh number curve corresponding to $\bar{R}_{TC}^{sub}$ is a prediction of the parallel flow approximation, i.e. a non-linear theory. Finally, the curves presented for the critical Hopf Rayleigh number, $\bar{R}_{TC}^{Hopf}$, result from the linear stability analysis of the convective flow predicted by the parallel flow approximation. The ($\bar{R}_{TC}$, φ) plane is divided into four quadrants. Region I (II) correspond to $j > -1.6$ and $\bar{R}_T > 0$ (<0), and IV (III) to $j < -1.6$ and $\bar{R}_T > 0$ (<0). According to Eq. (23), for $j = -1.6$, the critical Rayleigh number $\bar{R}_{TC}^{sup}$ for the onset of motion is equal to infinity. Also, it is observed from Fig. 7 that, for $j = -1.1$, three critical Rayleigh numbers, namely the supercritical, subcritical and oscillating Rayleigh numbers, coexist. The case of a layer heated from below (quadrant I and IV) will be discussed first. For this situation, since $\varphi > 0$, the solutal buoyancy forces induced by the Soret effect and the solute flux, j, are cooperative with the thermal buoyancy forces provided that $j > 0$. For $j < 0$ the solutal buoyancy forces resulting from the imposition of the solute flux j are in opposition with those resulting from both the heat flux and the Soret effect. Thus, upon decreasing gradually the value of j below zero, a value will be reached, namely $j = -1.1$, where the net solutal buoyancy forces will counteract the thermal ones. Thus, according to the linear stability theory in quadrant I, the onset of motion occurs through a supercritical Rayleigh number for $j > -1.1$. However, for $-1.6 < j < -1.1$, the non-linear parallel flow theory predicts the occurrence of a subcritical bifurcation. The same type of bifurcation prevails in region IV where, furthermore, the possible occurrence of oscillating flows ($\sigma = 0$) is predicted by the numerical analysis of the linear stability analysis discussed above. Since the buoyancy forces induced by the thermal and Soret effects are opposing those resulting from $j < 0$ in quadrant IV, the onset of convection occurs through a subcritical bifurcation. A comparison is made in Fig. 7 between the numerical predictions obtained with this latter, for the supercritical Rayleigh number, and the analytical solution, Eq. (23). The agreement between these two results is observed to be excellent. The case of a layer heated from above (quadrant II and III) will be now discussed. In region II, for $j > -1.6$ both the thermal and the net solutal buoyancy forces are stabilizing such that the system is unconditionally stable and the fluid at rest. For $j < -1.6$ the net solutal buoyancy forces are destabilizing while the thermal one are stabilizing. As a result, since the Lewis number is greater than unity, the onset of motion occurs through a supercritical Rayleigh number and not through a subcritical one. Also, the numerically determined Hopf's Rayleigh numbers are depicted in the graph for reference. A numerical test has been done to verify the validity of those results. The numerical code developed to solve the full governing equations has been run for the conditions $\varphi = 0.2$, $Le = 10$, $a = 1$, $A = 6$ and $Ra_T \approx 13{,}000$, i.e. at a Rayleigh number about 20% over the value $Ra_{TC}^{Hopf} = 10,782$ predicted by the linear stability theory. The resulting flow was observed to remain almost parallel, however the core of the cell was found to be slightly oscillating.

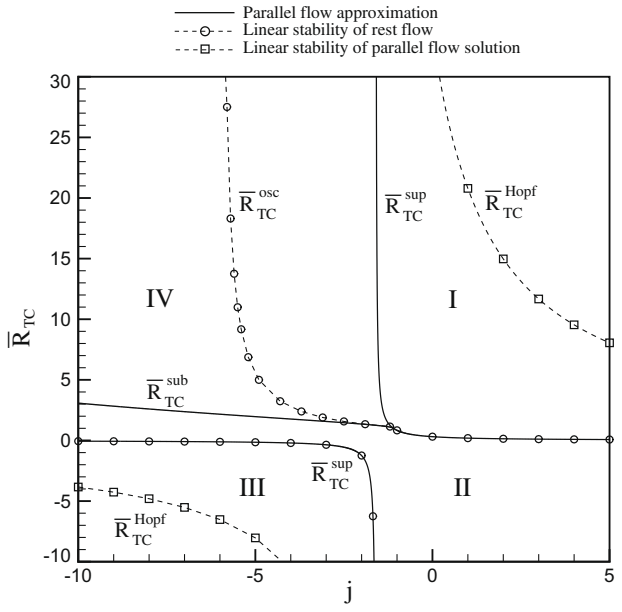

Fig. 7. Stability diagram in the ($\bar{R}_{TC}$, j)-plane for the case $Le = 10$, $\varphi = 0.2$ and $a = 1$.

6. Conclusions

In this paper an analytical and numerical study of natural convection in a shallow cavity, filled with a binary mixture, has been conducted. A constant heat flux was applied on the horizontal boundaries of the layer while the vertical ones were adiabatic. The solutal buoyancy forces were assumed to be generated by the combined action of the Soret effect and the imposition of a constant flux of concentration on the horizontal walls (double diffusive convection). Conditions for both aiding and opposing thermal and concentration buoyancy forces were examined for a large range of the governing parameters, namely, the thermal Rayleigh number Ra_T, the buoyancy ratio φ, the Lewis number Le, the Prandtl number Pr, the aspect ratio of the cavity A, the solute flux j, and the type of convection a. The main findings of the present investigation are as follows:

1. The onset of stationary supercritical and subcritical convection have been determined analytically in terms of the governing parameters of the problem, namely the buoyancy ratio φ, the Lewis number Le, the solute flux j and the constant a .
2. An analytical solution, based on the parallel flow approximation, has been derived for the case of an infinite layer ($A \gg 1$). The approximate model, despite its relative simplicity, predicts successfully the various types of flows encountered in the present study. This covers aiding flows and opposing flows.
3. A linear stability analysis of the parallel flow solution has been carried out and the threshold for Hopf's bifurcations, Ra_{TC}^{Hopf}, obtained numerically. In this way it has been possible to delineate the boundaries defining the regions of stationary and oscillatory instabilities.

A control volume method has been used to obtain a numerical solution of the full governing equations. A good agreement is observed between the analytical predictions and the numerical simulations.

Acknowledgements

This paper was performed while P. Vasseur was enjoying his stay in the laboratory of Professor A. Ambari from l'École Nationale Supérieure d'Arts et Métiers (ENSAM), Angers, France.

References

Baines, P.G., Gill, A.E., 1969. On the thermohaline convection with linear gradients. J. Fluid Mech. 37, 289–306.

Bennacer, R., Mahidjiba, A., Vasseur, P., Beji, H., Duval, R., 2003. The Soret effect on convection in a porous domain under cross temperature and concentration gradient. Int. J. Numer. Methods Heat Fluid Flow 13, 199–215.

Bhadauria, B.S., 2006. Temperature modulation of double diffusive convection in a horizontal fluid layer. Zeitschrift fur Naturforschung 61, 335–344.

DeGroot, S.R., Mazur, P., 1969. Non Equilibrium Thermodynamics. North-Holland Publisher, Amsterdam.

Huppert, H.E., Moore, D.R., 1976. Nonlinear double diffusive convection. J. Fluid Mech. 78, 821–854.

Huppert, H.E., Turner, J.S., 1981. Double diffusive convection. J. Fluid Mech. 106, 299–329.

Hurle, D.T.J., Jakeman, E., 1971. Soret-driven thermosolutal convection. J. Fluid Mech. 47, 667–687.

Kim, M.C., Choi, C.K., 2007. Analysis of onset of Soret-Driven convection by the energy method. Phys. Rev. E 76, 363021–363026.

Knobloch, E., Proctor, M., 1981. Nonlinear periodic convection in double-diffusive systems. J. Fluid Mech. 108, 291–316.

Larre, J.P., Platten, J.K., Chavepeyer, G., 1997. Soret effect in ternary systems heated from below. Int. J. Heat Mass Transfer 40, 545–555.

Mamou, M., Vasseur, P., 1999. Thermosolutal bifurcation phenomena in porous enclosures subject to vertical temperature and concentration gradients. J. Fluid Mech. 395, 61–87.

Mamou, M., Vasseur, P., Hasnaoui, M., 2001. On Numerical stability analysis on double diffusive convection in confined enclosures. J. Fluid Mech. 433, 209–250.

Nields, D.A., 1967. The thermohaline Rayleigh–Jeffreys problem. J. Fluid Mech. 29, 545–548.

Ouiriemi, M., Vasseur, P., Bahloul, A., 2005. Natural convection of a binary fluid in a slightly inclined shallow cavity. Numer. Heat Transfer 48, 547–565.

Ouiriemi, M., Vasseur, P., Bahloul, A., Robillard, L., 2006. Natural convection in a horizontal layer of a binary mixture. Int. J. Therm. Sci. 45, 752–759.

Patankar, S., 1980. Numerical Heat Transfer and Fluid Flow. Hemisphere, Washington, DC.

Platten, J.K., Chavepeyer, G., 1973. Oscillatory motion in Bénard cell due to the Soret effect. J. Fluid Mech. 60, 305.

Platten, J.K., Legros, J.C., 1984. Convection in Liquids. Springer, Berlin.

Proctor, M.R.E., 1981. Steady subcritical thermohaline convection. J. Fluid Mech. 29, 105.

Prud'homme, M., Hung Nguyen, T., 2002. Parallel flow stability under a uniform heat flux: effect of the Prandtl number. Int. Commun. Heat Mass Transfer 29, 749–756.

Schechter, R.S., Verlarde, M.G., Platten, J.K., 1974. The two components Bénard problem. Adv. Chem. Phys. 26, 265.

Sparrow, E.M., Goldstein, R.J., Jonsson, V.K., 1964. Thermal instability in a horizontal fluid layer: effect of boundary conditions and nonlinear temperature profile. J. Fluid Mech. 18, 513–528.

Trevisan, O., Bejan, A., 1985. Natural convection with combined heat and mass transfer buoyancy effects in a porous medium. Int. J. Heat Mass Transfer 28, 1597–1611.

Turner, J.S., 1985. Multi-component convection. Ann. Rev. Fluid Mech. 17, 11–44.

Veronis, G., 1965. On finite amplitude instability in thermohaline convection. J. Market Res. 23, 1–17.

Veronis, G., 1968. Effect of a stabilizing gradient of solute on thermal convection. J. Fluid Mech. 34, 315–368.